Thermo-Mechanical Modeling of Friction Stir Spot Welding and Numerical Solution With The Finite Element Method

Ahmet Atak, Aydın Şık, Veysel Özdemir

Abstract— **In this paper, friction stir spot welding (FSSW) of magnesium sheets were analyzed using finite element method (FEM). Various tool shoulder types used in Friction stir welding (FSW) were chosen as different parameter. Thermic simulations were showed that thermic conditions vary with tool shoulder design types used in friction stir welding. Heat energy input (Q) of numerical model was solved analytically and calculated based on the various parameter values. Friction factor surface pressure and materials thermic properties which are changing with generated heat during friction welding were also considered in the FEM analysis. Thermic field model was solved numerically and results were presented.**

Index Terms— **Friction stir spot welding (FSSW), Tool tip shoulder profile design, Magnesium welding, Thermal analysis of FSSW.**

I. INTRODUCTION

1.1. Importance, Problem and Purpose

Friction stir welding (FSW) of solid materials such as metals and polyethylene has a lot of significant advantages compare to fusion welding techniques such as [1, 2, 3]:

- Short welding time, shorter surface preparation time and easy to automate
- No fume and radiation emission during joining process
- No protective gas, powder and additional wire required
- No welding groove preparation required
- Welding possibility in almost all welding positions
- Improved mechanical properties (especially improved fatigue strength)
- Less retained stress and joining faults

Friction stir spot welding (FSSW) was derived from Friction stir welding (FSW) which is a new remarkable welding method used not only in automotive industry but also other industrial fields [4, 5]. Thanks to automation application, FSSW can be further developed by integrating to robot and automation systems. Therefore FSSW can enable efficient end lap joining in short process time [6, 7, 8].

Ahmet Atak, M.Sc., Gazi Üniversitesi/FBE/Endüstri Ürünleri Tasarımı ABD/Doctorate Student
Aydın Şık, Prof. Dr., Gazi Üniversitesi/Mimarlık Fakültesi /Endüstri Ürünleri Tasarımı Bölümü
Veysel Özdemir, Dr., Gazi Üniversitesi/Teknoloji Fakültesi/Endüstriyel Tasarım Mühendisliği Bölümü

Compare to other fusion welding techniques most significant benefit of FSSW technique is joining of work pieces without fusion of metal sheets and no welding wire required. FSSW set consists of stir tool tip and tool shoulder. Friction heat is generated through vertically moving and rotating tool set in defined time on the end lap positioned work pieces [9, 10, 11, 12]. The work piece softened and plastically deformed by means of the heat generated by rotating welding tool on the work piece. Solid state joining of top and bottom sheets is realized by moving back the welding set after defined time. Figure 1 shows that (a) the plunging of welding set to end lap positioned work pieces (b) joining (c) moving back the welding set.

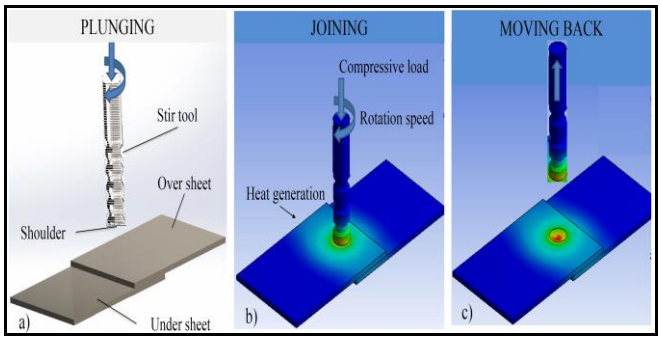

Figure 1: Graphic illustration of FSSW technique;

a) Penetration,

b) joining,

c) moving back

FSSW stir tool tip and tool shoulder design, diameter and length directly effects the stir movement and heating of joining pieces. Welding set tool tip geometry affects the welding seam formation and consequently alters the seam tensile strength. Joining operations with improper tool tip results with lower tensile strength and welding faults. Hence the tool sets used in FSSW and welding parameters are quite important [13, 14].
In this study, Joining of 2 mm thick magnesium sheets (AZ31) with stir tool tips having different shoulder profiles were thermally analyzed.

1.2. Method

In this study, Magnesium sheets were joined with FSSW technique by using tool tips having different shoulder design. Tool tip shoulder designs used in this study were shown in Figure 2 - a) and b).

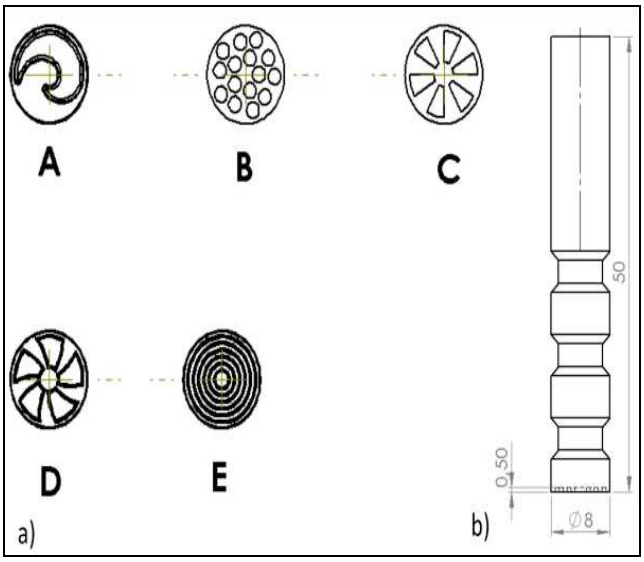

Figure 2: a) Designs of different shoulder profiles, **b)** Tool tip design

FSSW joining technique is principally conversion of mechanical energy to heat energy. Generated heat input was modelled analytically in thermo-mechanical model part. Calculated heat energy is the input parameter of numerical solution of the thermic field model with FEM. Thermal input depends with direct proportion to the stir tool tip diameter, rotation speed, compressive force and friction coefficient. During joining of sheets generated heat is also given to the ambient [15].

In this study, Numerical solution of thermic field model was obtained by using required thermal values and boundary conditions in FEM method. Chemical composition and mechanical properties of used AZ31D metal sheets are shown in and Table 2 [16].

Table 1: Chemical composition of used metal AZ31D (wt.%)

	Mg	Al	Zn	Mn	Si <	Fe	Cu <	Ni <	CA	Others
AZ31D	94–96	2.5–3.5	0.6–1.4	0.2–1.0	0.05	0.002	0.01	0.001	0.04	0.01

Table 2: Mechanical properties of metal AZ31D

	Yield strength [MPa]	Tensile strength [MPa]	Elongation [%]	Hardness HB
AZ31D	182	213	3.97	51.3

II. THERMO-MECHANICAL MODEL

Heat generation during FSSW welding is mainly affected by stir tool shoulder profile design, friction coefficient, compressive force and rotation speed [17]. Thermo-mechanical model and its parameters of heat (Q) which is generated by converting mechanical energy (P) produced through stir tool tip application onto the work piece are shown in figure 3.

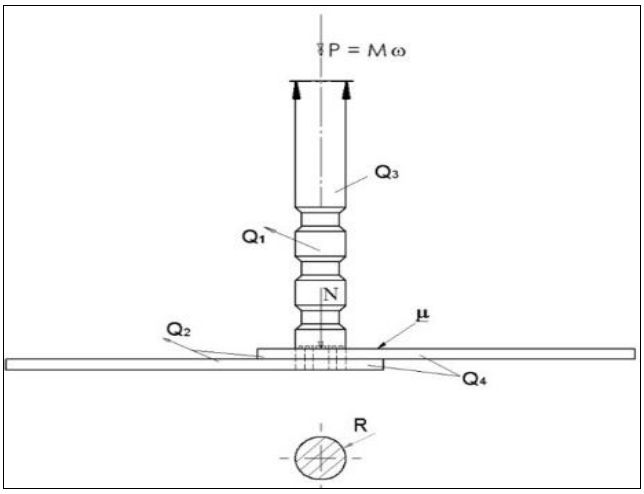

Figure 3: Thermo-mechanical model of heat generation in FSSW

Analytically calculated heat energy is the input parameter of the numerically solved thermic field model with FEM method. This thermal input is in direct proportion with the stir tip radius (R), rotation speed (ω), compressive force (N) and friction coefficient (μ). During joining heat content of sheets increase (Q_3 ve Q_4) and also some heat is released to the ambient(Q_1 ve Q_2). While the heat generated on the stir tool tip (Q_3) is desired to move away(Q_1), but the heat formed on the work piece (Q_4) to be quickly formed and preserved (Q_2) [18].

The equation of the conversion of mechanical energy to the heat energy of the model shown in Figure 3 can be expressed as below:

$$Q = P$$

In this equation (P) expresses the mechanical energy supplied by drive unit and (Q) generated total heat energy with the equation of$Q = Q_1 + Q_2 + Q_3 + Q_4$. The heat formed on the materials and exhausted heats to the ambient were solved numerically with FEM method. By considering transformation of mechanical energy to the heat energy (Q) the heat input value in the thermic model was obtained.

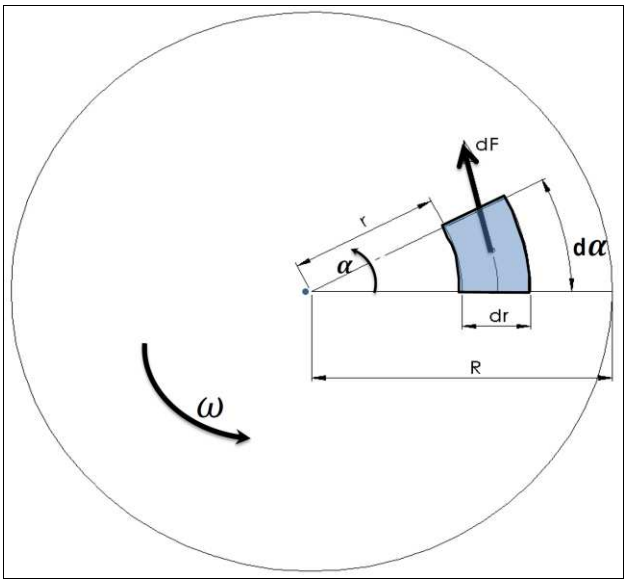

Figure 4: The infinitesimal area model on the mechanical friction surface in FSSW

The infinitesimal area model in Figure 4 can be expressed with the following equation:

$$dP = \omega\left(r+\frac{dr}{2}\right)dF = \omega\left(r+\frac{dr}{2}\right)\tau\, dr\left(r+\frac{dr}{2}\right)d\alpha = \omega\,\tau\left(r+\frac{dr}{2}\right)^2 dr\, d\alpha$$

If the square of the brackets calculated, the equation can be rearranged as:

$$dP = \omega\,\tau\left(r^2 + rdr + \frac{dr^2}{4}\right) dr\, d\alpha \quad (1)$$

When the differential equation no. (1) integrated twice with dr and rearranged:

$$dP = \omega\,\tau\left(r^2 + \frac{r^2}{2} + \frac{r^2}{8}\right) dr\, d\alpha \quad (2)$$

In this equation τ expresses the shear stress on the friction surface. When differential equation integrated for the radius and angle following equation is obtained.

$$P = \int_0^{2\pi}\int_0^R \omega\,\tau\left(r^2 + \frac{r^2}{2} + \frac{r^2}{8}\right) dr\, d\alpha = \frac{13R^3}{24}\,\omega\,\tau\int_0^{2\pi} d\alpha = \frac{13}{12}\pi\omega\tau R^3 \quad (3)$$

$\tau = \mu\frac{N}{A_c}$: Shear stress on friction surface (4)

$k_A = \frac{A_c}{A}$: Tool shoulder profile surface area ratio expresses the ratio of shoulder profile contact area to tool circular cross sectional area. This factor is defined to consider different shoulder profile designs. A_c expresses contact area and A tool circular cross sectional area. Based on these notations contact area can be expressed as:

$A_c = k_A A = k_A\,\pi\,R^2$ (5)

When the equations (4) and (5) rearranged in equation (3), below equation is obtained:

$$P = \frac{13}{12}\,\mu\,\frac{N}{k_A}\,\omega\,R \quad (6)$$

Here: $\mu = 0{,}5$: Heat dependent friction coefficient below melting point [24]

N : Vertical compressive force to welding area, selected as N=1848 Newton [25]

R : Stir tip radius, selected as R = 4 mm

P : Applied mechanical power through the drive unit in Watt

M : Applied mechanical moment through the drive unit in Nm= Joule

$\omega = 2\pi n$: Rotation speed; in this study average rotation selected as n= 2000 rpm = 33,3 Hz

Table 3 shows the k_A ratios used in this study in relation with tool shoulder profiles shown in Figure 2

Table 3: The shoulder profile area ratios

Tool Shoulder Profile Type	A	B	C	D	E
k_A	0,586	0,64	0,67	0,588	0,604
Average k_A	0,6				

Analytically developed heat formation equation (6) is conform to the equation developed by; Schmidt, Hattel and Wert [26]. Thermic field heat input is calculated thru equation (6) and above mentioned data. The calculation result can be shown as below:

$$Q = P = \frac{13}{12}\,\mu\,\frac{N}{k_A}\,\omega\,R = \frac{13}{12}\,0{,}5\,\frac{1848N}{0{,}6}\,2\,\pi\,33{,}3Hz\,0{,}004m = 1396\,W$$

III. NUMERICAL SOLUTION OF MODEL USING FEM

1.3. Thermic Load

Kinetic energy (P) supplied through the drive unit is converted to the heat energy (Q) through rotation of stir tool shoulder on the work piece [27, 28, 29, 30]. Equation (1) articulates the analytical model of this conversion. Heat input from the stir tool tip (Q) is in direct proportion with applied compressive force, rotation speed, and friction coefficient and stir tool tip radius. Since the average heat input in this study fluctuates insignificantly, it is considered in the calculation as Q= 1396W. There is linear heat input increase from center towards to outward of the stir tool tip. Also heat input is inverse proportion with shoulder profile contact ratio (k_A) to work piece.

1.4. Thermal Boundary Conditions and Material Parameters

Fast rotating stir tool tip cools down depending on its surface area through the heat emitting to the ambient. Heat transfer coefficient of outside of stir tool tip considered for calculation as $\alpha_1 = 30\ \frac{W}{m^2.{}^oC}$ [25]. Heat loss thru stir tool tip can be expressed as $Q_1 = \alpha_1 \Delta T_1 A_1$ (Figure 3). In this equation ΔT_1 states the temperature difference between stir tool tip and ambient. The temperature of the stir tool tip on the shoulder profile is desired to be high, but on the other hand other part of the stir tool tip temperature to be low so that the stir tool tip kept cooled. In order to increase the surface area of stir tool tip, its surface machined as trapezoidal form (Figure 2-b)). Another heat loss also occurs thru the metal sheets Q_2 to the ambience (Figure 3). Heat transfer coefficient for the air flow contacting with the welding pieces is considered as

$\alpha_2 = 15\ \frac{W}{m^2.^oC}$. [26]. Heat losses thru the welding piece can be expressed as $Q_2 = \alpha_2 \Delta T_2 A_2$ (Figure 3). In this equation ΔT_2 expresses the temperature difference between work piece and environment.

In this thermal analysis following heat capacities are considered in the calculation;

Heat capacity for steel $C_{p1} = 434\ \frac{J}{kg.^oC}$ and heat capacity for magnesium $C_{p2} = 1024\ \frac{J}{kg.^oC}$

Since the heat capacities do not vary significantly with the temperature, they are assumed constant. Thermal properties of workpieces can be seen in Table 4.

Table 4: Thermal properties of materials used in the model

Material:	Steel pin	Magnesium sheet
Heat transfer coefficient: $\alpha\ [\frac{W}{m^2.^oC}]$	30	10
Heat capacity: Cp [J/kg°C]	434	1024

1.5. Solution Method, Results and Interpretation

Thermal field model solved with FEM method and results are evaluated in below.

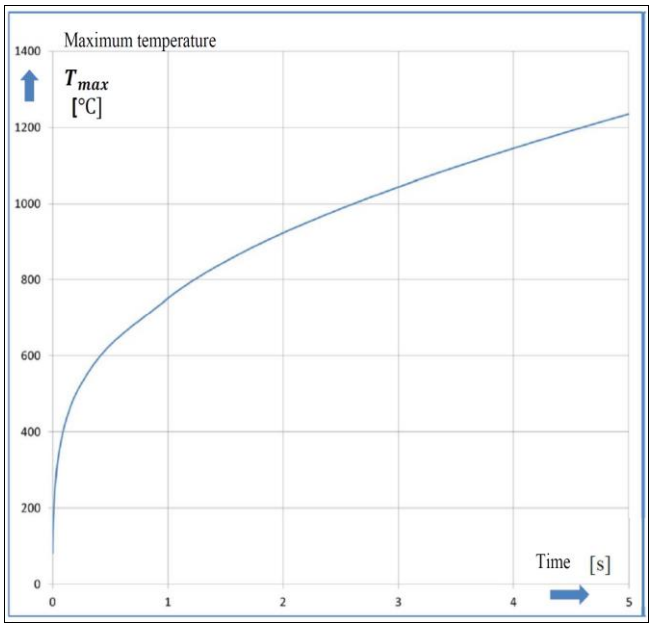

Figure 5: Numerical solution of maximum temperature development on the tool shoulder profile surface for shoulder profile type A

According to thermal analysis result theoretically tool shoulder profile surface temperature reaches 900 °C in 2 seconds after welding start as shown in Figure 5. High rotation speed of 2000 rpm and also small tool tip diameter of 8 mm are the reason for such a quick temperature increase of 900 °C in 2 seconds after welding start. However, such a high temperature practically cannot be reached, since the friction coefficient of 0,5 decreases with the increasing material temperature and reaches almost 0 at melting temperature of work pieces. Since the stir tool tip rotates with very high speed, it is impractical to measure temperature on the welding spot. Thus the definition of friction coefficient with changing temperature is impractical. As the friction coefficient decreases with the increasing temperature, stir tool tip temperature reaches the melting temperature of work piece which is 650 °C.

Welding temperature of 650 °C is very high for stir tool tip material which is structural steel (St 52) even if the welding time of 2 seconds is very short. In order to overcome this problem, there are some studies to cool down the stir tool tip actively, but these are expensive and cannot cool down effectively the stir tool. Hence the effective passive cooling measures, which can be introduced during industrial manufacturing of stir tool tip, are suggested such as increase of side surface area of stir tool tip and using of heat resistant structural steels.

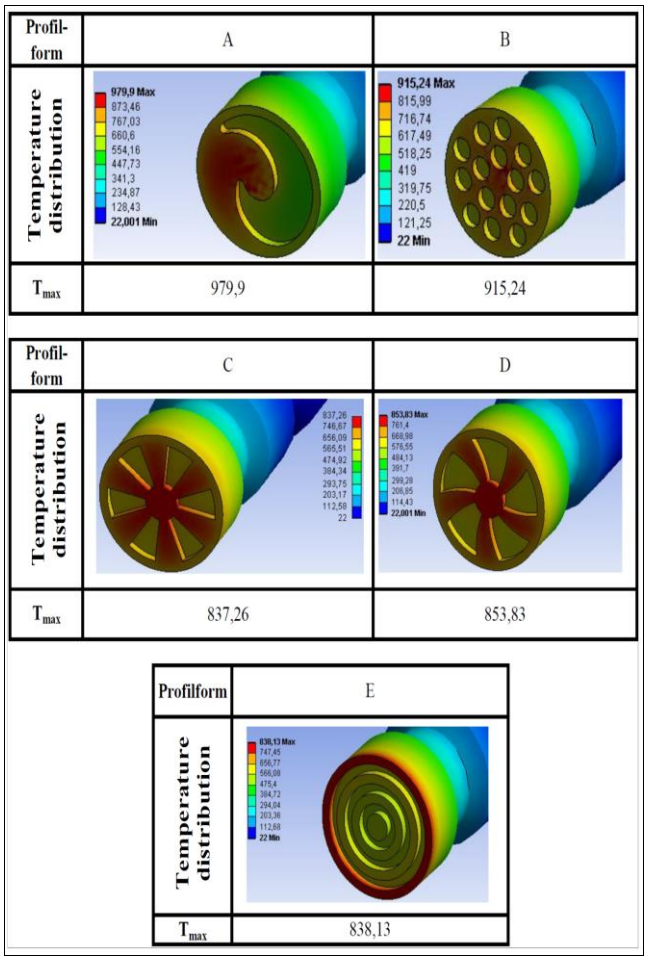

Figure 6: The temperature distribution of stir tool tips in the shoulder profiles after 2 seconds.

Temperature distribution after 2 seconds after welding start on the stir tip shoulder profile was shown in Figure 6. One can see that the highest temperature was reached on shoulder profile B and D. This is caused by regular tool shoulder profile which is aimed.

Peak temperature of magnesium sheets reaches to 600 °C in average within 2 seconds after welding start with the shoulder profile type A. The maximum heat flux density appears to be achieved at 4 mm stir tool tip radius, which is the maximum value of the radius of the shoulder as expected and 2 seconds after welding start.

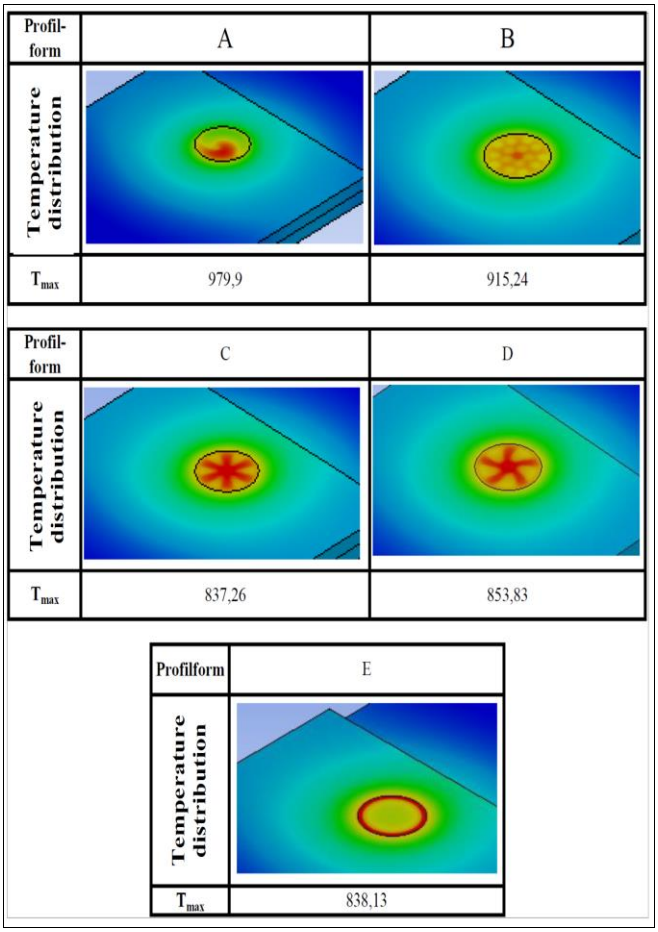

Figure 7: The temperature distribution on the Magnesium plates 2 seconds after welding start.

Figure 7 shows the temperature distribution on magnesium plates 2 seconds after welding start for various tool shoulder profiles types. One can see that the highest surface temperature reached on tool shoulder profile A and B. However, the most homogeneous temperature distribution which affects the welding quality was reached with the tool shoulder profile type B.

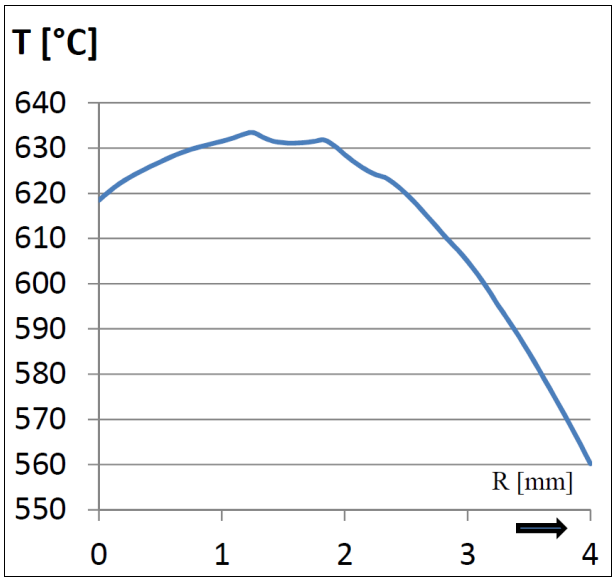

Figure 8: Temperature distribution 2 seconds after welding start on tool shoulder profile type A; from welding center to outwards.

As it can be seen in Figure 8, while the temperature rises to 618 ° C and 632 ° C at a distance of up to 30% of the radius from the center to the periphery, it shows a parabolic drop towards to the profile wall and reaches down to 560 ° C on the profile wall. It is seen that the material temperature changes in inverse proportion to the square root of the stir tool tip radius.

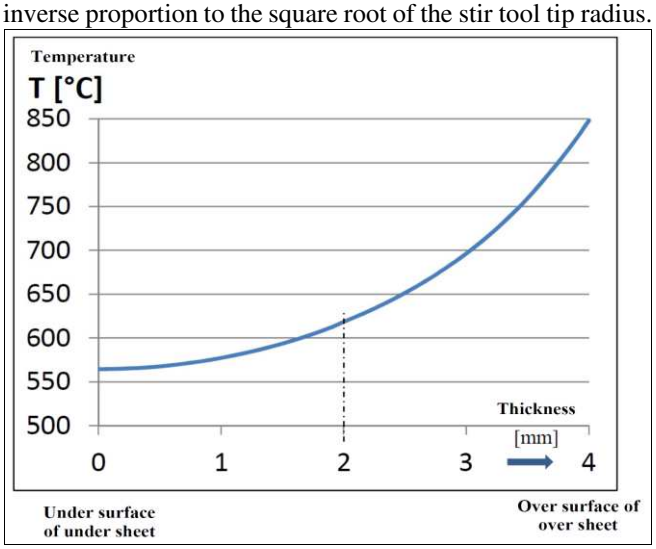

Figure 9: In the case of shoulder profile type A; Temperature distribution after 2 seconds from bottom surface to top surface depending on thickness

As it can be seen in Figure 9, the temperature arises from 560°C at bottom surface of plates to the top of the plates 850 °C. It is seen that material temperature shows a parabolic changes with the plate thickness.

IV. CONCLUSIONS

In this study; the value of the heat energy which will used in the numerical analysis was calculated according to various parameters and the following results were obtained:

1. It was seen that results are changing with stir tool tip shoulder profile parameter accordingly.
2. It was seen that the highest surface temperature 2 seconds after welding start were reached on tool shoulder profile A and B.
3. It was found out that tool shoulder profile B and D has the most homogenous distribution profiles 2 seconds after welding which can affect the welding start quality accordingly.
4. It was seen that the material temperature reached in 2 seconds after welding start 600°C.
5. It was found out that the highest heat value was reached on outer wall of the tool shoulder profile 2 seconds after welding start.

REFERENCES

[1] ŞIK A., KAYABAŞ Ö., Sürtünme karıştırma kaynağı ile yapılan Alüminyum kaynağında kaynak bölgesinin mekanik özelliklerinin incelenmesi, Gazi Üniversitesi Endüstriyel Sanatlar Eğitim Fakültesi Dergisi, Y.11, S.12, 30-43, 2003.

[2] ŞIK A., Sürtünme Karıştırma Kaynağı İle Birleştirilen Magnezyum Levhaların Mekanik Özelliklerinin İncelenmesi, SAÜ. Fen Bilimleri Dergisi, 14. Cilt 14, Sayı 2, 134-140, 2010

[3] FENG Z., DİAMOND S., SANTELLA M. L., PAN T. Y., and Li N., High strength weight reduction materials-Friction stir welding

(FSW)and processing of advanced materials, Oak Ridge National Laboratory Report DE-AC05-00OR22725, 101-108, 2004.
[4] MITLIN D., RADMILOVIC V., PAN T., CHEAN J., FENG Z., and SANTELLA, M., L., Structure properties relations in spot friction welded (also known as friction stir spot welding) 6111 aluminum, Mater. Sci. and Eng., 441, 79-96, 2006.
[5] LIYANAGE T., KILBOURNE J., GERLICH A. P. & NORTH T. H., Joint formation in dissimilar Al alloy/steel and Mg alloy/steel friction stir spot welds, Science and Technology of Welding and Joining, 14:6, 500-508, 2013
[6] SANTELLA M. L., GRANT G. J., FENG Z., CARPENTER J. A., SKLAD P. S., Friction stir spot welding of high strength steel, Oak Ridge National Laboratory & Pacific Northwest National Laboratory Progress Report, DE-AC05-00OR22725 & DE-AC06-76RLO1830, 336-339, 2005.
[7] BUFA G., FRATINI L., PIACENTINI M., Tool path design in friction stir spot welding of AA6082-T6 aluminum alloys, Key Engineering Materials, 344, 767-774, 2007.
[8] ROSENDO T., MAZZAFERRO J., MAZZAFERRO C., TIER M., RAMOS F., REGULY A., STROHAECKER T., DOS SANTOS J. (2013). Friction Spot Processes - FSSW and FSpW, http://www.hzg.de/imperia/md/content/gkss/institut_fuer_werkstofffforschung/wmp/posterapresentacao-gkss2.pdf, visit date: 28 March 2013
[9] SU P, GERLICHA, NORTH TH, BENDZSAK GJ. "Friction Stir Spot Welding of Aluminum and Magnesium Alloys". Materials Forum, 29, 290-294, 2005.
[10] KÜLEKÇİ M. K., ŞIK A., Kaluç E. "Effects of Tool Rotation and Pin Diameter on Fatigue Properties of Friction Stir Welded Lap Joints". The International Journal of Advanced Manufacturing Technology, 36(9), 877-882, 2008.
[11] BOZKURT Y, BİLİCİ M. K. "Application of Taguchi Approach to Optimize of FSSW Parameters on Joint Properties of Dissimilar AA2024-T3 and AA5754-H22 Aluminum Alloys". Materials and Design, 51, 513-521, 2013.
[12] TOZAKI Y., UEMATSU Y., TOZAKI K., "Effect of Tool Geometry on Microstructure and Static Strength in Friction Stir Spot Welded Aluminium Alloys", International Journal Machine Tools Manufacture, 47, 2230-2236, 2007.
[13] LATHABAI S., PAINTER M. J., CANTIN G. M. D., TYAGI V. K., "Friction Spot Joining of an Extruded Al-Mg-Si alloy", Scripta Materialia, 55(10), 899-902, 2006.
[14] BİLİCİM. K., BAKIR B., BOZKURT Y., ÇALIŞ İ., "Sürtünme karıştırma nokta kaynak tekniği ile birleştirilen farklı alüminyum levhaların taguchi analizi", Pamukkale Univ Muh Bilim Derg, 22(1), 17-23, 2016
[15] KAFALI H., AY N., Havacılıkta Kullanılan 6013-T6 Alüminyum Alaşımının Sürtünme Karıştırma Kaynağıyla Birleştirilmesi, Süleyman Demirel Üniversitesi Fen Bilimleri Enstitüsü Dergisi, 18(1), 38-47, 2014
[16] ŞIK A., Comparison between microstructure characteristics and joint performance of AZ31 magnesium alloy welded by TIG and Friction stir welding (FSW)(FSW) processes, Kovove Material 51, 197–203, 2013
[17] SHIN H.-S. & DE LEON M., Weldability assessment of friction stir spot welded lightweight alloys using pin and pinless tools, Science and Technology of Welding and Joining, 21:2, 99-105, 2016
[18] ŞIK A., Otomobil saclarının MIG/MAG kaynağında gaz karışımlarının bağlantının mekanik mekanik özelliklerine etkisi, Gazi Üniversitesi Endüstriyel Teknoloji Eğitimi, Doktora tezi, 2002.
[19] LIU Z., CUI H., JI S., XU M., MEN X., Improving Joint Features and Mechanical Properties of Pinless Fiction Stir Welding of Alcald 2A12-T4 Aluminum Alloy, Journal of Materials Science & Technology, V. 32, 1372–1377, 2016
[20] CHIOU Y.-C., LIU C. T., LEE R.-T., A pinless embedded tool used in FSSW and FSW of aluminum alloy, Journal of Materials Processing Technology, V. 213, 1818–1824, 2013
[21] Chu Q., YANG X. W., LI W. Y. & LI Y. B., Microstructure and mechanical behaviour of pinless friction stir spot welded AA2198 joints, Science and Technology of Welding and Joining, 21:3, 164-170, 2016
[22] WENYA L., JINFENG L., ZHIHAN Z., DALU G., WEIBING W., GUOHONG L., Pinless Friction stir welding (FSW)of AA2024-T3 Joint and Its Failure Modes, Tianjin University and Springer-Verlag Berlin Heidelberg, V. 20, 439-443, 2014
[23] SIMONCINI M., CICCARELLI D., FORCELLESE A., PIERALISI M., Micro- and Macro- Mechanical Properties of Pinless Friction Stir Welded Joints in AA5754 Aluminium Thin Sheets, Science Direct (Available online at www.sciencedirect.com 2212-8271) Procedia CIRP 18, 9–14, 2014
[24] BAKAVOS D., CHEN Y., BABOUT L. AND PRANGNELL P., Material Interactions in a Novel Pinless Tool Approach to Friction Stir Spot Welding Thin Aluminum Sheet, The Minerals Metals & Materials Society and ASM International, METALLURGICAL AND MATERIALS TRANSACTIONS A, Volume 42A, 1266-1282, 2011
[25] Klobčar D. & Tušek J. & Smolej A. & Simončič S., Parametric study of FSSWof aluminium alloy 5754 using a pinless tool, International Institute of Welding, Weld World, V.59, 269–281, 2015
[26] CHEN C., KOVACEVIC R., Thermomechanical modelling and force analysis of Friction stir welding (FSW)by the finite element method, Journal of Mechanical Engineering Science (online version: http://pic.sagepub.com/content/218/5/509), 218-509, 2004
[27] HIRASAWA S., BADARINARAYAN H., OKAMOTO K., TOMIMORA T. , KAWANAMI T., Analysis of effect of tool geometry on plastic flow during friction stir spot welding using particle method, Journal of Materials Processing Technology, V. 210, 1455–1463, 2010
[28] SU P., GERLICH A., NORTH T. H. & BENDZSAK G. J., Energy utilisation and generation during friction stir spot welding, Science and Technology of Welding and Joining, 11:2, 163-169, 2006
[29] CHIOU Y.-C., LIU C.-T., LEE R-T., A pinless embedded tool used in FSSW and FSW of aluminum alloy, Journal of Materials Processing Technology, V. 213, 1818–1824, 2013
[30] GERLICH A., SU P., NORTH T. H ., Tool penetration during friction stir spot welding of Al and Mg alloys, JOURNAL OF MATERIALS SCIENCE, V. 40, 6473–6481, 2005
[31] SCHMIDT H., HATTEL J., An analytical model for the heat generation in friction stir welding, Modelling and simulation in materials science and engineering, V.12, 143-157, 2004
[32] JABER JWEEG M., HAMEED TOLEPHIH M., ABDUL-SATTAR M., Theoretical and experimental investigation of transient temperature distribution in Friction stir welding (FSW)of AA 7020-T53, Journal of Engineering, N. 6, V. 18, 2012